

OpenObject-NAV: Open-Vocabulary Object-Oriented Navigation Based on Dynamic Carrier-Relationship Scene Graph

Yujie Tang¹, Meiling Wang¹, Yanan Deng^{1†}, Zibo Zheng^{2†}, Jiagui Zhong^{1†}, Yufeng Yue^{1*}

Abstract—In everyday life, frequently used objects like cups often have unfixed positions and multiple instances within the same category, and their carriers frequently change as well. As a result, it becomes challenging for a robot to efficiently navigate to a specific instance. To tackle this challenge, the robot must capture and update scene changes and plans continuously. However, current object navigation approaches primarily focus on semantic-level and lack the ability to dynamically update scene representation. This paper captures the relationships between frequently used objects and their static carriers. It constructs an open-vocabulary Carrier-Relationship Scene Graph (CRSG) and updates the carrying status during robot navigation to reflect the dynamic changes of the scene. Based on the CRSG, we further propose an instance navigation strategy that models the navigation process as a Markov Decision Process. At each step, decisions are informed by Large Language Model’s commonsense knowledge and visual-language feature similarity. We designed a series of long-sequence navigation tasks for frequently used everyday items in the Habitat simulator. The results demonstrate that by updating the CRSG, the robot can efficiently navigate to moved targets. Additionally, we deployed our algorithm on a real robot and validated its practical effectiveness. The project page can be found here: <https://OpenObject-Nav.github.io>.

I. INTRODUCTION

With the advancement of visual language models (VLM) [1] and large language models (LLM) [2], the realization of cognitive navigation [3] has attracted increasing attention. Imagine a daily environment, a robot is expected to navigate efficiently to any object, whether it is static furniture or a frequently used object with changing positions (such as a cup). This necessitates the robot to represent and update the current state of objects in the scene and navigate to the target.

Current object navigation methods [4]–[13] can effectively navigate to static objects (like a sofa). However, they are often limited to searching for semantic-level objects and lack the capability to update scenes. Hence, when it comes to frequently used daily items such as a “*cup on the black table*,” these objects typically come in various colors and styles. They may appear in places such as the kitchen, bedroom, and others, and their positions are not fixed. Additionally, they are usually carried by other objects, meaning that the carriers are also not fixed. Such navigation targets are highly

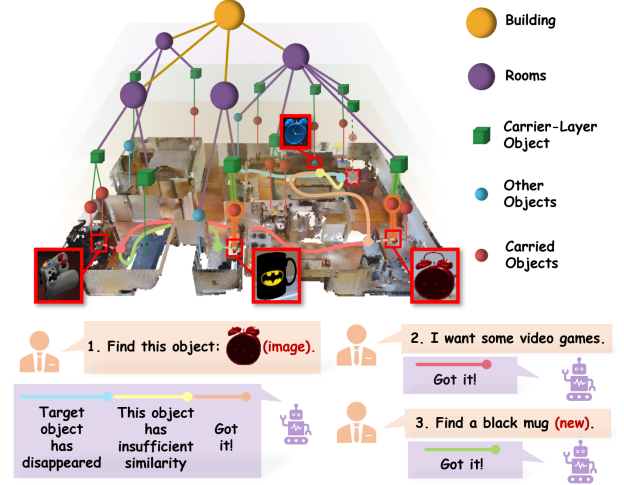


Fig. 1. The robot executes long-sequence, multi-modal, and multi-type daily object navigation commands based on a dynamic carrier-relationship scene graph. **First**, it successfully navigates to the displaced **red alarm clock**, eliminating interference from a **blue alarm clock** of the same type along the way. **Next**, based on the user’s request, it navigates to a **game controller**. During these tasks, the robot observes a new **black cup**, which is added to the scene graph. This update enables efficient point-to-point navigation for the **third** task.

dynamic and subject to interference, making it challenging to efficiently and effectively navigate to them.

To appropriately represent highly dynamic and interference-prone daily environments and achieve more efficient navigation to everyday objects, an appropriate hierarchical scene representation is essential. Current scene representation methods [14]–[20] have already constructed hierarchical scene graphs. However, they struggle to represent everyday dynamic environments due to two key challenges. First, their graph structures fail to capture the relationships between static objects and frequently moved everyday items. Second, frequently used daily objects often have changing positions and repetitive semantics, making efficient updates more difficult. Considering that frequently used objects are typically carried by static ones, this article distinguishes between static carriers and the objects they carry. We leverage LLM and VLM to identify these static carriers and construct an open-vocabulary carrier-relationship scene graph (CRSG), which effectively represents the carrying relationships between objects. In the process of robot navigation, new observations are matched with carrier objects in the carrier layer. For the observed carrier objects, dynamic updates are performed to reflect

This work is supported by the National Natural Science Foundation of China under Grant No. NSFC 62233002, 62003039. (Corresponding Author: Yufeng Yue, yueyufeng@bit.edu.cn)

¹Yujie Tang, Meiling Wang, Yanan Deng, Jiagui Zhong, Yufeng Yue are with School of Automation, Beijing Institute of Technology, Beijing, 100081, China.

²Zibo Zheng are with School of Mechanical Engineering, University of Nottingham Ningbo China, Ningbo, 315100, China.

†: Equal contribution.

any changes in the everyday objects they carry.

Based on the CRSG, we designed an object-oriented navigation strategy, modeling the object search process as a Markov Decision Process (MDP) [21]. At each navigation step, the robot decides to navigate toward candidate target objects or unexplored carrier objects based on visual-language feature similarities and the commonsense knowledge from the LLM, until the target is found.

In summary, our contributions are as follows:

- We present an adaptable carrier relationship scene graph (CRSG) that primarily describes the dynamic carrier and carried relationships between objects.
- We design a navigation strategy based on the CRSG, utilizing visual-language features and commonsense knowledge from the LLM to inform decision-making.
- Extensive qualitative and quantitative experiments demonstrate that our method effectively navigates to long sequences of moved objects, and the effectiveness of updating CRSG has been validated. Additionally, we deployed and tested the algorithm on a real robot, confirming its practicality.

II. RELATED WORK

A. Open Vocabulary Mapping

With the advent of vision-language models like CLIP [22] and its variants, scene mapping with different representations has moved beyond the limitations of fixed classes [23], [24], and expanded to open-vocabulary [19], [25]–[29]. Clip-fields [30] integrates CLIP and SBERT features into the neural implicit map, enabling open-vocabulary map queries and navigation for robots. VLMap [31] and IVLMap [32] project CLIP features top-down onto a 2D grid to enable zero-shot (instance) vision-language navigation. ConceptGraph [19] and Hovsg [20] constructed instance-level point cloud maps with CLIP features embedded and scene graph representing certain relationships between objects, which facilitates more detailed and precise object retrieval.

These maps provide crucial support for applications such as open-vocabulary object queries, scene understanding, and robot navigation. However, they do not have dynamic update capabilities. We construct a carrier-relationship scene graph (CRSG) that describes the dynamic carrier and carried relationships between objects, and continuously updating the CRSG during navigation. This helps achieve more efficient navigation of everyday objects.

B. Object Navigation

Object navigation [4]–[13], [33], as one of the key tasks in the field of embodied intelligence, primarily involves navigating to a specified semantic or instance location within a scene. [4]–[9] mainly perform object navigation within the close-classes. [19], [20], [32] constructed an offline instance map of the scene, enabling zero-shot instance navigation. [10]–[13] perform open-vocabulary object navigation using the frontier exploration method. However, they [10]–[13], [19], [20], [32] cannot capture changes in the positions of frequently used objects, or the addition and removal of instances

in the scene. [33] involves object navigation within close-classes and similarly does not involve scene updates. We have built a dynamic open vocabulary CRSG that not only supports semantic object navigation but also enables efficient navigation to everyday instances (such as a red cup) that are spatially variable and subject to semantic interference. The approach most similar to ours is GOAT [34], which also implements memory capabilities for the latest scene and supports multi-type and multi-modal navigation command inputs. However, for navigating to a displaced everyday object, we have designed a navigation strategy based on CRSG, while GOAT selects the closest unexplored region to navigate to the object.

III. METHOD

A. Problem Definition

In a daily environment, when given a navigation command, the robot queries the CRSG to determine the navigation end-point and proceeds to the specified destination. If the target is a daily item (e.g., a cup) that is being carried, the robot evaluates whether the item remains in its original location based on the current observations. If not, the robot initiates a strategic exploration process. We define this challenge as a **displaced object exploration and navigation task** within an everyday setting. An overview of the system framework is provided in Fig. 2. The cost function is defined as follows:

$$P.L = \sum_{t=1}^T \text{Length}(L_t, L_{t+1}) \quad (1)$$

Let L_t represent the position of the exploration target at step t , and $\text{Length}(L_t, L_{t+1})$ denote the shortest path between L_t and L_{t+1} , calculated by using path planning algorithms. Additionally, T represents the number of exploration attempts the robot makes to navigate to the target object. We aim to minimize $P.L$ in Eq. (1).

B. Carrier-Relationship Scene Graph (CRSG)

We first construct an open-vocabulary instance map \mathcal{M} using the pre-collected RGB-D data of the scene. Unlike ConceptGraph [19], each instance object $\mathbf{O}_i \in \mathcal{O}$ (\mathcal{O} is the set of all objects) not only contains a CLIP feature $\mathbf{V}\mathbf{F}_i$ but also stores a caption description list \mathbf{cap}_i generated from the Tokenize Anything model [35] and text feature $\mathbf{T}\mathbf{F}_i$ encoded with SBERT model [36]. A Carrier-Relationship Scene Graph (CRSG) $\mathcal{S.G}$ is then constructed below.

Building and Room layer: Existing works, such as [16], [20], propose various methods for room segmentation. We select specific point clouds from \mathcal{M} and project them onto the $x - y$ plane: wall point clouds within a certain height range from the ground, and “door” point clouds filtered using captions and text features. Next, we apply the line-search method, inspired by [37], to identify closed contours for each room, assigning objects within these contours to their corresponding rooms. The combined room layers constitute the building layer.

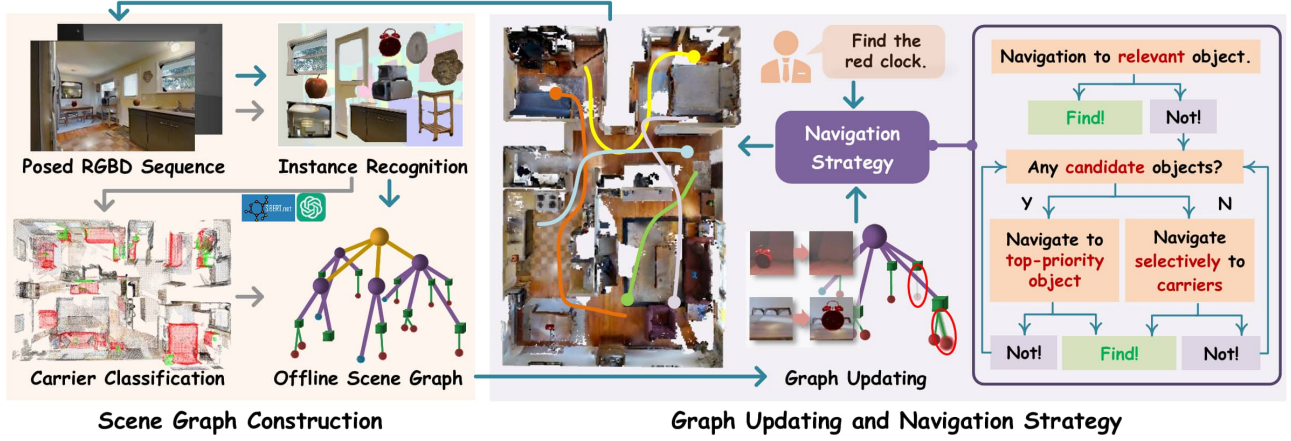


Fig. 2. The OpenObject-NAV system framework consists of two main modules. The Scene Graph Construction module focuses on constructing the carrier-relationship scene graph. The Graph Updating and Navigation Strategy module is responsible for executing cognitive navigation based on user instructions, following the proposed navigation strategy, while updating the scene graph in the process.

Carrier layer: We calculate the similarity between the text features $T \cdot F_i$ of each object O_i and the SBERT-encoded text feature \tilde{T} for “furniture for holding objects”. The mathematical expression for this is as follows.

$$\text{sim}(T \cdot F_i, \tilde{T}) = \frac{T \cdot F_i \cdot \tilde{T}}{\|T \cdot F_i\| \|\tilde{T}\|} \quad (2)$$

Next, we select the set of objects $\tilde{O} \subseteq O$ with a similarity score exceeding a specified threshold σ , as shown below.

$$\tilde{O} = \{(O_i, \text{cap}_i, T \cdot F_i) | \text{sim}(T \cdot F_i, \tilde{T}) > \sigma\} \quad (3)$$

Next, we extract the three most frequent captions for each cap_i in \tilde{O} , input them into a LLM (GPT-4o for test), and use a specific prompt to identify potential carrier-type objects, denoted as $\tilde{O}_1 \subseteq \tilde{O}$.

Finally, we select the final set of carrier-layer objects, denoted as $\bar{O} \subseteq \tilde{O}_1$, based on criteria such as the objects’ geometric dimensions exceeding a certain size and their contact with the ground, as shown below.

$$\bar{O} = f(\tilde{O}_1) \quad (4)$$

Object layer: For any non-carrier-layer object $O_i \in (O - \bar{O})$, we determine whether O_i is carried by a carrier-layer object $O_j \in \bar{O}$ based on O_i ’s dimensions, the closest distance, and the spatial overlap relationship in the x-y-z directions between O_i and O_j (exceeding a certain overlap rate). $h(O_j, O_i)$ is defined to encapsulate the consideration of the aforementioned factors, where $h(O_j, O_i) = 1$ if all the conditions are satisfied. For any $O_j \in \bar{O}$, we define the set of objects $C(O_j)$ carried by O_j as follows:

$$C(O_j) = \{O_i | h(O_j, O_i) = 1, O_i \in (O - \bar{O})\} \quad (5)$$

C. Navigation Strategy for a Displaced Object

Let the **input navigation command** for the target object be either a *text*, or an *image*. *text* or *image* is encoded using the SBERT or CLIP model, respectively. The resulting

feature is then compared with the SBERT or CLIP features of each object in the CRSG S_G using cosine similarity, similar to Eq. (2). The object with the highest similarity score is selected as the target object, O_{target} .

We model the exploration of a displaced object as a fixed-policy Markov decision process (MDP) below.

state space S : In the current step t , we define:

1. the robot’s pose $L_t \in \mathcal{L}$,
2. the set of unexplored carrier-layer objects $CR_t \in \mathcal{CR}$,
3. the set of candidate target objects *on the unexplored carrier-layer objects* $CT_t \in \mathcal{CT}$,
4. the flag of finding the target or not $F_t \in \{0, 1\}$. (\mathcal{L} , \mathcal{CR} and \mathcal{CT} denote the value set of L_t , CR_t and CT_t respectively.)

The state variable S_t is defined in (6).

$$S_t = (L_t, CR_t, CT_t, F_t) \in S \quad (6)$$

In the initial state $S_0 = (L_0, CR_0, CT_0, F_0)$, L_0 is the initial position of the robot, $CR_0 = \bar{O}$, and $CT_0 = O_{\text{target}}$.

action space A :

$$A = \{\text{Stop}, \text{Explore}(cr), \text{Goto}(ct) \mid cr \in CR_t, ct \in CT_t\} \quad (7)$$

Stop indicates that the task is completed or all carrier-layer objects have been explored. *Explore*(cr) and *Goto*(ct) represent exploring the carrier-layer object $cr \in CR_t$ and navigating to the location of $ct \in CT_t$, respectively.

The robot selects the next action $a_t \in A$ based on the current state S_t according to a specific policy $\pi(\cdot)$ in (8).

$$a_t = \pi(S_t) \quad (8)$$

policy $\pi(\cdot)$: Given current state $S_t = (L_t, CR_t, CT_t, F_t)$,

1. if $F_t = 1$ or $CR_t = \emptyset$, then $a_t = \text{Stop}$.

2. If $F_t = 0$ and $CT_t \neq \emptyset$, we prioritize and select a candidate object to proceed with. Specifically, let $CT_t = \{O_{t1}, \dots, O_{ti}\}$. Some additional variables are stored: the SBERT similarities $SS_t = \{ss_{t1}, \dots, ss_{ti}\}$ between CT_t and O_{target} , the distances $D_t = \{d_{t1}, \dots, d_{ti}\}$ between L_t and

CT_t , and the average depth values $\tilde{D}_t = \{\tilde{d}_{t1}, \dots, \tilde{d}_{ti}\}$ when CT_t are observed by the robot's camera. The priority rating of any $\mathbf{O}_{tj} \in CT_t$ corresponding to ss_{tj} , d_{tj} and \tilde{d}_{tj} , is evaluated as follows. The parameters in (9) are set as $\omega_1 = 3$, $\alpha = 0.1$ and $\omega_2 = 1$ in the experiments.

$$P_R(\mathbf{O}_{tj}) = \frac{\omega_1 \cdot ss_{tj} \cdot \exp(-\alpha \tilde{d}_{tj})}{1 + \omega_2 \cdot d_{tj}} \quad (9)$$

Where ss_{tj} is positively correlated with $P_R(\mathbf{O}_{tj})$, as we assume that a larger ss_{tj} indicates a higher likelihood that the candidate is the target. Moreover, \tilde{d}_{tj} is negatively correlated with $P_R(\mathbf{O}_{tj})$, based on the assumption that the accuracy of the front-end detection model decreases as \tilde{d}_{tj} increases. Therefore, $\exp(-\alpha \tilde{d}_{tj})$ is considered the confidence level of ss_{tj} . The robot will navigate to the location of the object with the maximum P_R and explore for \mathbf{O}_{target} .

3. If $F_t = 0$, $CT_t = \emptyset$ and $CR_t \neq \emptyset$, the LLM selects one of the carrier objects $cr_k \in CR_t$ and the robot executes the action $a_t = Explore(cr_k)$. Specifically, the captions for each carrier object in CR_t are extracted and provided as input to the LLM, along with the image or caption of the target object. Leveraging the LLM's commonsense understanding of object-carrier relationships (e.g., “a cup is unlikely to be placed on a toilet”), the LLM identifies the carrier object where the target object is most likely to be found.

state transition process: If $a_t = Explore(cr)$ (where $cr \in CR_t$) or $a_t = Goto(ct)$ (where $ct \in CT_t$), then during the robot's movement, let $CR_{observed}$ represent the set of carrier objects observed within a small radius r that have no candidate targets on them (based on the latest environmental observations), and let CT_{new} represent the set of new target candidates found on unexplored carrier objects. Since some candidates in CT_t may be carried by objects in $CR_{observed}$, CT_t is updated to CT_t^* after these candidates are removed. Specifically, the candidates in CT_{new} are those for which the SBERT feature similarities with the target exceed a threshold σ_1 . Additionally, the similarities between the target \mathbf{O}_{target} and the objects carried in $CR_{observed}$ don't exceed σ_1 .

1. if $a_t = Explore(cr)$, CR_{t+1} and CT_{t+1} are updated as:

$$CR_{t+1} = CR_t \setminus (\{cr\} \cup CR_{observed}) \quad (10a)$$

$$CT_{t+1} = CT_t^* \cup CT_{new} \quad (10b)$$

2. if $a_t = Goto(ct)$, CR_{t+1} and CT_{t+1} are updated as:

$$CR_{t+1} = CR_t \setminus (\{cr_1\} \cup CR_{observed}), \quad ct \in C(cr_1) \quad (11a)$$

$$CT_{t+1} = CT_t^* \cup CT_{new} \setminus \{ct\} \quad (11b)$$

In either case, the SBERT feature similarities between \mathbf{O}_{target} and the objects carried by cr or cr_1 are calculated. If the input command is an image, an LLM-based image comparison is also performed. If the combined score from the LLM's image comparison and the SBERT text similarity for a carried object exceeds σ_2 , then $F_{t+1} = 1$, and the task is marked as complete.

TABLE I
SUCCESS RATE OF OBJECT QUERY ON AN OUTDATED OFFLINE MAP

Method	scene_1	scene_2	scene_3	SR
VLMaP	7/14	8/19	7/17	44%
ConceptGraph	9/14	10/19	12/17	62%
Ours	13/14	15/19	15/17	86%

D. CRSG Adaptation

Matching carrier objects. As the robot navigates, it periodically captures RGB and depth images from the environment. The RGB images are processed through CropFormer [38], Tokenize Anything model [35], CLIP [22] and SBERT [36] to obtain instance masks, captions, encoded CLIP features and encoded SBERT features, respectively. For newly observed objects, the robot compares them with the carrier objects in S_G to identify the observed carrier objects \mathbf{O}_{match}^{cr} . The primary aspects of comparison include the object's size, the distance between their center positions, and the similarity scores based on CLIP and SBERT features.

The Addition or Removal of Carried Objects. For currently observed instances, $h(\cdot, \cdot)$ in Eq. (5) is used to determine whether they are being carried by \mathbf{O}_{match}^{cr} . Let the set of carried objects in the new observations be defined as \mathbf{O}^{crd} . The previously carried objects on \mathbf{O}_{match}^{cr} are then compared with \mathbf{O}^{crd} . The criteria also include the object's size, the distance between center positions, and the SBERT feature similarity score. After the comparison, the carried objects on \mathbf{O}_{match}^{cr} are updated accordingly: they are either added, removed, or left unchanged.

IV. EXPERIMENTAL RESULTS

We aim to answer the following research questions:

1. Does the carrier-relationship scene graph (CRSG) improve the accuracy of instance object queries (Sec. IV-A)?
2. Does the dynamic update of the CRSG contribute to more efficient instance navigation (Sec. IV-B, IV-C)?

Metrics. We report Success Rate(SR) and Success weighted by inverse Path Length (SPL) [39]. SPL measures the efficiency of an robot's path by comparing it to the shortest route from the starting point to the target object instance. If the robot fails to reach the target, the SPL score is zero. Otherwise, the score is calculated as the ratio of the shortest path length to the robot's actual path length, with higher values indicating better performance.

A. Object Query on the Outdated Offline Map

We compare the object query accuracy of scene representations with those of VLMaP [31] and ConceptGraph [19]. A total of 50 queries with different types of navigation instructions (semantic, instance and requirement-driven) were conducted across 3 scenes in Gibson [40]. The experimental results are presented in Tab. I, where our object query success rate averages 86% and is the highest in all three scenarios. Because in instance queries like “a cup on the table”, the CRSG we constructed records the carrying relationship between *cup* and *table*, thus allowing

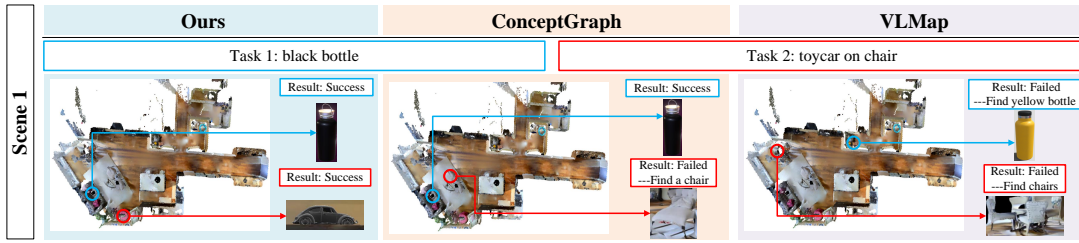


Fig. 3. Static Object Query Experiment: Comparison of Target Object Query Results on the Offline Map.

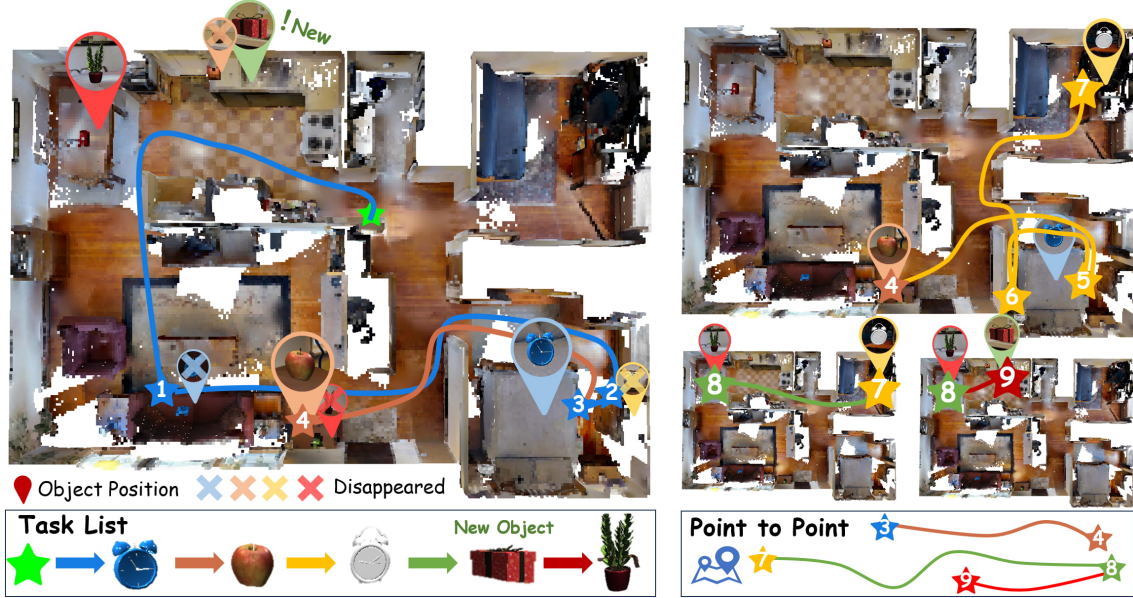


Fig. 4. The visualization of a long-sequence instance navigation result in scene 2 is shown, where "Point to Point" represents the shortest path navigation.

for precisely locating the instance. In contrast, VLMap [31] and ConceptGraph [19] may find the *table* instead of the *cup*. Besides, we additionally incorporate text features of caption descriptions for each object in CRSG, demonstrates superior performance in differentiating between similar objects, such as *black cup* and *white cup*. Meanwhile, VLMap projects the CLIP features from 3D space to a 2D grid, and its queryable semantic types are limited, resulting in inferior performance. We illustrate partial query results of different methods in Fig. 3, and the results demonstrate that our method performs better in distinguishing between objects of the same category and in querying carried instances.

B. Long-sequence Navigation Task for Frequently Used Everyday Items

We conducted a series of long-sequence frequently used daily items navigation experiments (4 or 5 objects as a sequence) in three everyday scenarios in Gibson [40] using the Habitat navigation simulator [41]. In each scene, we placed a variety of frequently used items from different instances (like black cup, blue alarm clock, plastic bottle, game controller and so on), while offline constructing the CRSG for each scene. We set up multiple distractor objects of the same category (like black / white cup) to validate our

ability to correctly navigate to a specific instance. We then randomly altered the positions of these items to simulate the variability in the locations of commonly used everyday objects. Next, the robot is instructed to sequentially navigate to these objects in each scene.

We present the navigation results for each scene in Tab. II for SR and Tasks_SR(i), and Fig. 5 for SPL. Tasks_SR(i) represents the success rate of correctly navigating to all i objects. We also presented SR in Tab. II when using only SBERT feature similarity (**ours-Text**) and GPT-4o (**ours-LLM**) for image matching to determine targets. Tab. II shows that **ours** achieves generally the highest SR and Tasks_SR(i). This indicates that considering both SBERT feature similarity and the image matching results from GPT-4o contributes to navigating to the true-positive target. Fig. 4 illustrates an example of long-sequence navigation, where the efficiency of navigating to the target significantly improves as the number of navigated objects increases. Additionally, as shown in Fig. 5, the SPL for the first object is noticeably lower, while the SPL for the remaining objects shows significant improvement. Since the process of navigating to the first object involves multiple explorations, it often results in a navigation path length that greatly exceeds the shortest path. During this period, the observed CRSG is updated, enabling

TABLE II

SR AND TASKS_SR(i) IN DIFFERENT SCENES FOR A SERIES OF LONG-SEQUENCE FREQUENTLY USED DAILY ITEMS NAVIGATION TASKS

Object	SR (%) / Tasks_SR(i) (%)								
	scene_1			scene_2			scene_3		
	ours-Text	ours-LLM	ours	ours-Text	ours-LLM	ours	ours-Text	ours-LLM	ours
1	68.8 / 68.8	75.0 / 75.0	81.3 / 81.3	53.8 / 53.8	84.6 / 84.6	84.6 / 84.6	73.3 / 73.3	86.7 / 86.7	100 / 100
2	56.3 / 37.5	68.8 / 50.0	75.0 / 56.3	76.9 / 53.8	100 / 84.6	100 / 84.6	100 / 73.3	60.0 / 46.7	100 / 100
3	68.8 / 31.3	56.3 / 25.0	75.0 / 31.3	84.6 / 46.2	76.9 / 61.5	76.9 / 61.5	100 / 73.3	60.0 / 13.3	100 / 100
4	81.3 / 18.8	87.5 / 25.0	100 / 31.3	69.2 / 23.1	92.3 / 53.8	84.6 / 46.2	100 / 73.3	66.7 / 6.7	73.3 / 73.3
5	61.5 / 23.1	69.2 / 15.4	76.9 / 30.8	44.4 / 0	66.7 / 33.3	66.7 / 33.3	100 / 62.5	50.0 / 0	100 / 62.5

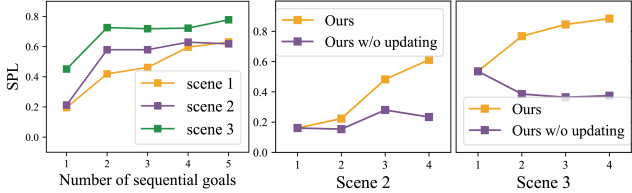


Fig. 5. The **first** figure presents the SPL results in Sec. IV-B, while the **second** and **third** figures show the results of the ablation experiments with and without CRSG updates in Sec. IV-C.

TABLE III
ABLATION STUDY: SPL OF SINGLE OBJECT NAVIGATION

Metric	only-carriers_Random	only-carriers_LLM	ours
SPL	0.205	0.309	0.342

the positions of other objects to be refreshed. As a result, when navigating to the remaining objects (including new instances), point-to-point navigation is primarily achieved, leading to an increase of SPL.

C. Ablation Study

To further investigate the role of CRSG updates in efficient navigation to everyday objects, we conducted ablation experiments on one long-sequence navigation tasks in each of Scene 2 and Scene 3, comparing cases with and without CRSG updates. The results (in Fig. 5, second and third figures) indicate that when CRSG is updated, the SPL gradually increases, while there is no improvement in SPL without CRSG updates. Thus, the updates to CRSG contribute to more efficient navigation to displaced everyday objects.

We also conducted single daily object navigation experiments in three different scenes to evaluate the impact of various modules in our navigation strategy on navigation efficiency. **only-carriers_Random** represents navigating to a randomly selected carrier object for exploration, without considering candidate target objects. **only-carriers_LLM** selects the next carrier object for exploration based on LLM's recommendations, building upon **only-carriers_Random**. As shown in Tab. III, our method achieves the highest SPL, followed by **only-carriers_LLM**. This indicates that the strategy of navigating to candidate target objects and selecting the carrier objects to explore based on the commonsense knowledge of LLM contributes to more efficient navigation.

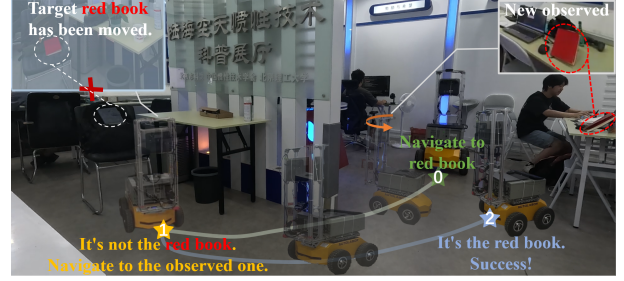


Fig. 6. The robot queries the CRSG for the position of the **red book** at the **chair** and navigates there. It then discovers that the red book is not in its original location and rules out the interference of the **grey book**. Finally, it navigates to the **newly observed** position of the red book.

D. Real-World Validation

We validated our algorithm using an Autolabor robot in a real scene, equipped with an industrial computer featuring an NVIDIA GeForce RTX 3080. We equipped the robot with a Livox Mid 360 LiDAR and utilized the Cartographer SLAM algorithm [42] to obtain its global pose. Additionally, an Azure Kinect DK was mounted to capture RGB-D information. The robot successfully navigates to a displaced red book shown in Fig. 6.

V. CONCLUSIONS

This paper has proposed an open-vocabulary navigation method for frequently used everyday items, leveraging a dynamic carrier-relationship scene graph (CRSG). Specifically, we first construct the CRSG to capture the dynamic relationships between carrier objects and the objects they carry. Next, a navigation strategy based on the CRSG is developed to navigate to frequently used items, modeling the object search process as a Markov Decision Process (MDP). At each navigation step, the CRSG is dynamically updated based on the robot's observations of the environment. The robot then decides whether to navigate toward candidate target objects or unexplored carrier objects, guided by visual-language feature similarities and commonsense knowledge from the LLM. Both simulations and physical experiments demonstrate that our method efficiently navigates to objects that are subject to positional changes, even in the presence of distractors from the same category. In the future, we plan to incorporate an online mapping module and parallel processing to improve exploration efficiency.

REFERENCES

- [1] J. Zhang, *et al.*, “Vision-language models for vision tasks: A survey,” *IEEE Transactions on Pattern Analysis and Machine Intelligence*, 2024.
- [2] Y. Chang, *et al.*, “A survey on evaluation of large language models,” *ACM Transactions on Intelligent Systems and Technology*, vol. 15, no. 3, pp. 1–45, 2024.
- [3] Y. Bai, *et al.*, “A review of brain-inspired cognition and navigation technology for mobile robots,” *Cyborg and Bionic Systems*, vol. 5, p. 0128, 2024.
- [4] M. Chang, *et al.*, “Semantic visual navigation by watching youtube videos,” *Advances in Neural Information Processing Systems*, vol. 33, pp. 4283–4294, 2020.
- [5] J. Ye, *et al.*, “Auxiliary tasks and exploration enable objectnav,” *arXiv preprint arXiv:2104.04112*, 2021.
- [6] D. S. Chaplot, *et al.*, “Object goal navigation using goal-oriented semantic exploration,” *Advances in Neural Information Processing Systems*, vol. 33, pp. 4247–4258, 2020.
- [7] H. Luo, *et al.*, “Stubborn: A strong baseline for indoor object navigation,” in *2022 IEEE/RSJ International Conference on Intelligent Robots and Systems (IROS)*, pp. 3287–3293. IEEE, 2022.
- [8] S. K. Ramakrishnan, *et al.*, “Poni: Potential functions for object-goal navigation with interaction-free learning,” in *Proceedings of the IEEE/CVF Conference on Computer Vision and Pattern Recognition*, pp. 18 890–18 900, 2022.
- [9] J. Zhang, *et al.*, “3d-aware object goal navigation via simultaneous exploration and identification,” in *Proceedings of the IEEE/CVF Conference on Computer Vision and Pattern Recognition*, pp. 6672–6682, 2023.
- [10] V. S. Dorbala, *et al.*, “Can an embodied agent find your “cat-shaped mug”? llm-based zero-shot object navigation,” *IEEE Robotics and Automation Letters*, 2023.
- [11] J. Chen, *et al.*, “How to not train your dragon: Training-free embodied object goal navigation with semantic frontiers,” *arXiv preprint arXiv:2305.16925*, 2023.
- [12] K. Zhou, *et al.*, “Esc: Exploration with soft commonsense constraints for zero-shot object navigation,” in *International Conference on Machine Learning*, pp. 42 829–42 842. PMLR, 2023.
- [13] N. Yokoyama, *et al.*, “Vlfm: Vision-language frontier maps for zero-shot semantic navigation,” in *2024 IEEE International Conference on Robotics and Automation (ICRA)*, pp. 42–48. IEEE, 2024.
- [14] A. Rosinol, *et al.*, “Kimera: From slam to spatial perception with 3d dynamic scene graphs,” *The International Journal of Robotics Research*, vol. 40, no. 12–14, pp. 1510–1546, 2021.
- [15] Y. Tian, *et al.*, “Kimera-multi: Robust, distributed, dense metric-semantic slam for multi-robot systems,” *IEEE Transactions on Robotics*, vol. 38, no. 4, 2022.
- [16] N. Hughes, *et al.*, “Hydra: A real-time spatial perception system for 3D scene graph construction and optimization,” 2022.
- [17] Y. Chang, *et al.*, “Hydra-multi: Collaborative online construction of 3d scene graphs with multi-robot teams,” in *2023 IEEE/RSJ International Conference on Intelligent Robots and Systems (IROS)*, pp. 10 995–11 002. IEEE, 2023.
- [18] N. Hughes, *et al.*, “Foundations of spatial perception for robotics: Hierarchical representations and real-time systems,” *The International Journal of Robotics Research*, p. 02783649241229725, 2024.
- [19] Q. Gu, *et al.*, “Conceptgraphs: Open-vocabulary 3d scene graphs for perception and planning,” in *2024 IEEE International Conference on Robotics and Automation (ICRA)*, pp. 5021–5028. IEEE, 2024.
- [20] A. Werby, *et al.*, “Hierarchical open-vocabulary 3d scene graphs for language-grounded robot navigation,” *Robotics: Science and Systems*, 2024.
- [21] F. Garcia, *et al.*, “Markov decision processes,” *Markov Decision Processes in Artificial Intelligence*, pp. 1–38, 2013.
- [22] A. Radford, *et al.*, “Learning transferable visual models from natural language supervision,” in *International conference on machine learning*, pp. 8748–8763. PMLR, 2021.
- [23] Y. Deng, *et al.*, “Hd-ccsom: Hierarchical and dense collaborative continuous semantic occupancy mapping through label diffusion,” in *2022 IEEE/RSJ International Conference on Intelligent Robots and Systems (IROS)*, pp. 2417–2422. IEEE, 2022.
- [24] Y. Deng, *et al.*, “S-mki: Incremental dense semantic occupancy reconstruction through multi-entropy kernel inference,” in *2022 IEEE/RSJ International Conference on Intelligent Robots and Systems (IROS)*, pp. 3824–3829. IEEE, 2022.
- [25] K. M. Jatavallabhula, *et al.*, “Conceptfusion: Open-set multimodal 3d mapping,” *arXiv preprint arXiv:2302.07241*, 2023.
- [26] S. Peng, *et al.*, “Openscene: 3d scene understanding with open vocabularies,” in *Proceedings of the IEEE/CVF conference on computer vision and pattern recognition*, pp. 815–824, 2023.
- [27] S. Lu, *et al.*, “Ovir-3d: Open-vocabulary 3d instance retrieval without training on 3d data,” in *Conference on Robot Learning*, pp. 1610–1620. PMLR, 2023.
- [28] Y. Deng, *et al.*, “Opengraph: Open-vocabulary hierarchical 3d graph representation in large-scale outdoor environments,” *arXiv preprint arXiv:2403.09412*, 2024.
- [29] Y. Deng, *et al.*, “Openobj: Open-vocabulary object-level neural radiance fields with fine-grained understanding,” *arXiv preprint arXiv:2406.08009*, 2024.
- [30] N. M. M. Shafiullah, *et al.*, “Clip-fields: Weakly supervised semantic fields for robotic memory,” *arXiv preprint arXiv:2210.05663*, 2022.
- [31] C. Huang, *et al.*, “Visual language maps for robot navigation,” in *2023 IEEE International Conference on Robotics and Automation (ICRA)*, pp. 10 608–10 615. IEEE, 2023.
- [32] J. Huang, *et al.*, “Ivlmap: Instance-aware visual language grounding for consumer robot navigation,” *arXiv preprint arXiv:2403.19336*, 2024.
- [33] A. Rajvanshi, *et al.*, “Saynav: Grounding large language models for dynamic planning to navigation in new environments,” in *Proceedings of the International Conference on Automated Planning and Scheduling*, vol. 34, pp. 464–474, 2024.
- [34] M. Chang, *et al.*, “Goat: Go to any thing,” *arXiv preprint arXiv:2311.06430*, 2023.
- [35] T. Pan, *et al.*, “Tokenize anything via prompting,” *arXiv preprint arXiv:2312.09128*, 2023.
- [36] N. Reimers, “Sentence-bert: Sentence embeddings using siamese bert-networks,” *arXiv preprint arXiv:1908.10084*, 2019.
- [37] T. Qin, *et al.*, “The maze method for extracting boundary lines.” <https://zhuanlan.zhihu.com/p/391392970>, 2021.
- [38] L. Qi, *et al.*, “High-quality entity segmentation,” *arXiv preprint arXiv:2211.05776*, 2022.
- [39] P. Anderson, *et al.*, “On evaluation of embodied navigation agents,” *arXiv preprint arXiv:1807.06757*, 2018.
- [40] F. Xia, *et al.*, “Gibson env: Real-world perception for embodied agents,” in *Proceedings of the IEEE conference on computer vision and pattern recognition*, pp. 9068–9079, 2018.
- [41] M. Savva, *et al.*, “Habitat: A platform for embodied ai research,” in *Proceedings of the IEEE/CVF international conference on computer vision*, pp. 9339–9347, 2019.
- [42] B. Xu, *et al.*, “Research of cartographer laser slam algorithm,” in *LIDAR Imaging Detection and Target Recognition 2017*, vol. 10605, pp. 49–57. SPIE, 2017.